Accepted Manuscript

Improving the reach of vaccines to low-resource regions, with a needle-free vaccine delivery device and long-term thermostabilization

Xianfeng Chen, Germain J.P. Fernando, Michael L. Crichton, Christopher Flaim, Sally R. Yukiko, Emily J. Fairmaid, Holly J. Corbett, Clare A. Bover, Alexander B. Ansaldo, Ian H. Frazer, Lorena E. Brown, Mark A.F. Kendall

PII: S0168-3659(11)00111-8
DOI: doi: 10.1016/j.jconrel.2011.02.026
Reference: COREL 5775

To appear in: *Journal of Controlled Release*

Received date: 8 December 2010
Accepted date: 23 February 2011

Please cite this article as: Xianfeng Chen, Germain J.P. Fernando, Michael L. Crichton, Christopher Flaim, Sally R. Yukiko, Emily J. Fairmaid, Holly J. Corbett, Clare A. Bover, Alexander B. Ansaldo, Ian H. Frazer, Lorena E. Brown, Mark A.F. Kendall, Improving the reach of vaccines to low-resource regions, with a needle-free vaccine delivery device and long-term thermostabilization, *Journal of Controlled Release* (2011), doi: 10.1016/j.jconrel.2011.02.026

Improving the reach of vaccines to low-resource regions, with a needle-free vaccine delivery device and long-term thermostabilization

Xianfeng Chen[1ξ], Germain JP Fernando[1ξ], Michael L Crichton[1], Christopher Flaim[1], Sally R Yukiko[1], Emily J Fairmaid[2], Holly J Corbett[1], Clare A Bover[1], Alexander B Ansaldo[1], Ian H Frazer[3], Lorena E Brown[2], Mark AF Kendall[1,3*]

[1]The University of Queensland, Delivery of Drugs and Genes Group (D^2G^2), Australian Institute for Bioengineering and Nanotechnology, Brisbane, QLD 4072, Australia

[2]The University of Melbourne, Department of Microbiology & Immunology, Parkville, VIC 3010, Australia

[3]The University of Queensland, The Diamantina Institute, Brisbane, QLD 4102, Australia

[ξ]These authors contributed equally to the work. [*]Correspondence author: m.kendall@uq.edu.au

Abstract

Dry-coated microprojections can deliver vaccine to abundant antigen-presenting cells in skin and induce efficient immune responses and the dry-coated vaccines are expected to be thermostable at elevated temperatures. In this paper, we show that we have dramatically improved our previously reported gas-jet drying coating method and greatly increased the delivery efficiency of coating from patch to skin to from 6.5% to 32.5%, by both varying the coating parameters and removing the patch edge. Combined with our previous dose sparing report of influenza vaccine delivery in mouse model, the results show that we now achieve equivalent protective immune responses as intramuscular injection (with the needle and syringe), but with only 1/30th of the *actual* dose. We also show that influenza vaccine coated microprojection patches are stable for at least 6 months at 23 ºC, inducing comparable immunogenicity with freshly coated patches. The dry-coated microprojection patches thus have key and unique attributes in ultimately meeting the medical need in certain low-resource regions with low vaccine affordability and difficulty in maintaining "cold-chain" for vaccine storage and transport.

Keywords: microprojection; vaccine coating; thermostability

1. INTRODUCTION

More than 17 million people die every year from infectious diseases – most of these in developing countries [1]. Many of the diseases could be prevented by vaccination, but vaccines are underutilized in low-resource regions. With all vaccines being sensitive to heat, the 'cold-chain' is essential for maintaining their quality during transport and storage [2]. This is a huge burden in vaccination campaigns. The cold-chain alone can contribute up to 80% of the financial cost of vaccination programs in developing countries [3].

Advances are being made to improve vaccine thermal stability, but they primarily still rely on the needle and syringe for delivery [2,4] – which hinders safe and effective vaccination, particularly in the developing world. For example, most vaccines delivered by needle and syringe into muscle, where there are relatively few professional antigen presenting cells in comparison with skin and lymph nodes. Therefore, high doses of vaccines are usually required, making vaccination even less affordable. Also needle-based vaccine delivery in low-resource regions is held back by the need for qualified medical practitioners, needle-stick injuries, unsafe injections, and disposal costs. For example, WHO estimates that up to one-third of immunization injections are unsafe in four of six regions of the world due to needle reuse, use of unsterilized needles, dangerous infections, etc [5]. In some regions, needles that deliver medication or vaccines become the vectors for spreading the diseases which they are designed to prevent.

To help address these social/medical problems, one very attractive and promising way is to use needle-free skin vaccine delivery. Central to this is: our skin contains an extensive network of

resident professional antigen-presenting cells, which have the capacity to capture the delivered vaccine, migrate to draining lymph nodes and orchestrate potent systemic immune responses [6-10]. Therefore, delivering vaccines to skin is expected to work more effectively than the traditional routes by needle and syringe. Using needle-free delivery routes can avoid needle-stick injuries, unsafe injections because of needle reuse and also the disposal costs.

Vaccines can be targeted into the skin by breaching the tough outer layer, called the stratum corneum. To meet this delivery challenge, many approaches are being actively investigated such as diffusion/permeation delivery, electroporation [11], biolistic microparticle delivery (Gene Gun) [12]. Each of these delivery routes has merit, but is also hindered by important disadvantages. For example: the physical barrier of the skin, the stratum corneum, only allows small molecules (<500 Da) to permeate the skin, but many target immunotherapeutics (e.g. vaccines) have much higher molecular weight (e.g. a few tens thousand to millions Da). The permeation/diffusion can be improved by adding chemical enhancers [13,14] or formulating in a nanogel form [15]. However, with these methods, the diffusion/permeation may take a long time when the molecular size is large and the delivery efficiency is usually low. In addition, it is difficult to accurately control the dose. The clinical use of electroporation and biolistic microparticle delivery is mainly hindered by the high cost of the device. Also, biolistic delivery is hindered by the high sensitivity of the ballistic penetration process to obvious and subtle variation in skin properties [16] and high cell death [17]. The electroporation process causes pain and discomfort to patients [18-20].

Alternatively, microprojection arrays are a vaccine delivery technology with several advantages over existing approaches [21-26]. Firstly, microprojection arrays can mechanically pierce the stratum corneum and deliver vaccines to the skin where there are large populations of antigen-presenting cells [21,26]. Secondly, microprojections can deliver a wide range of molecules (e.g. protein and DNA vaccines, virus like particles, drugs) without causing pain [23,25]. Thirdly, one of the most important hypotheses for the coated microprojections is that the dry-coating formulation will greatly enhance the thermostabilization of molecules, compared to when they are in a liquid state. However, to our knowledge, no successful study on the long term thermostability of dry-coated microprojection patches has been reported.

In this paper, we use a type of microprojection patch with different design from others in this field. Our microprojection patch, termed Nanopatch (NP) [27], designed 'from the ground up' for the purpose of delivering vaccines to skin. The NP contains very small and densely packed projections (21,025 projections per cm^2) for skin targeted vaccine delivery. We designed this device using a probability analysis [27] to target vaccine directly to thousands of the skin's APCs. We expected that our uniquely designed densely packed microprojections can greatly improve the vaccine efficacy. The details have been previously described [27]. The contained microprojections are clearly distinct from the large and sparsely packed "microneedles" reported in literature (up to 700 µm in length and less than 321 projections per cm^2) [23,24,28]. One of the key challenges for vaccine delivery to skin by these microprojections is coating the surface with vaccine – because of their extremely high packing density. We set about meeting this need by developing a gas-jet drying coating method to coat vaccines on the very small and densely packed microprojections [29]. The coating and NP technology has been tested to deliver a herpes virus type 2 DNA vaccine [30,31] and a seasonal influenza vaccine (Fluvax® 2008) in mouse model [27]. With the herpes virus type 2 DNA vaccine delivery, the results showed that microprojections can deliver the DNA vaccine to the skin and achieve comparable antibody responses and statistically equal protection rate against an HSV-2 virus challenge, when compared with the mice immunized with intramuscular injection using needle and syringe, but with less than 1/10th of the delivered antigen [30,31]. In influenza vaccine delivery, the results showed that, associated with physically targeting vaccine to thousands of antigen presenting cells in the skin, over 100 times less antigen was needed to be delivered to the skin to achieve an equivalent response when compared with intramuscular injection by needle and syringe. This represents a marked improvement – an order of magnitude greater than reported by others – without reliance on an added adjuvant and with only a single vaccination. This confirmed

our expectation of designing the densely packed microprojections for vaccine delivery. However, in the report, the influenza vaccine delivery efficiency (i.e. delivery dose into skin / full dose of coated patch) from patch into skin was only about 6.5%. This made the *actual* dose sparing only about 6 times despite the greatly enhanced vaccine efficacy.

The objectives of this paper are to: (1) significantly increase the coating delivery efficiency from microprojections to skin, to reduce the *actual* dose of vaccine per vaccination; and (2) investigate the long term thermostability of influenza vaccine dry-coated microprojection patches. Herein, we show that we have greatly increased the delivery efficiency of coating to 32.5%, by both altering the vaccine coating parameters and removing the patch edge. Furthermore, we also show that influenza vaccine coated NPs are stable for at least 6 months at 23 ºC, inducing comparable immunogenicity with freshly coated patches. Overall, we show, by experiment, that the NP has key and unique attributes in ultimately meeting the medical need in certain low-resource regions.

2. EXPERIMENTAL DETAILS

2.1 Materials

Methylcellulose (MC, the viscosity of 2 wt% MC in water is 55 mPa·S) and trehalose were purchased from Sigma-Aldrich (Castle Hill, NSW, Australia). Fluospheres (F8811, 0.2 micron yellow-green fluorescent particles) was ordered from Invitrogen. We used the seasonal human influenza vaccine, Fluvax2008® (CSL Ltd, Parkville Australia), which contains 15 μg hemagglutinin (HA) per 0.5 ml of each of the three viral strains bearing the surface antigens of A/Brisbane/10/2007 (H3N2), A/Solomon Islands/3/2006 (H1N1) and B/Florida/4/2006. Methyl ^{14}C-OVA was purchased from BioScientific Pty Ltd (Kirrawee, NSW, Australia).

2.2 NP fabrication

NP was fabricated from silicon using a process of Deep Reactive Ion Etching in Rutherford Appleton Laboratory, Oxford, UK [29]. The microprojections are solid silicon, sputter coated with a thin layer of gold (~ 100 nm in thickness). The morphology of microprojection patches and the associated vaccine coating were characterized by a JEOL scanning electron microscope 6400 or 6460LA. All samples reported in this paper were tilted at 45˚ for scanning electron microscopy (SEM).

2.3 Penetration study of microprojection patch on skin

Each patch was applied to the inner earlobe with a velocity of 2 m/s and a force of 0.6 N by a custom spring-loaded plunger based applicator device [32]. The mouse ears were freshly cut from the live mice and used within 10 minutes. The NP and skin assembly was then slush frozen in liquid nitrogen and transferred to a cryo-preservation chamber under vacuum. Then the assembly was sectioned with a knife in the vacuum chamber and sputter coated with a thin (approximately 5 nanometres) layer of gold for avoiding charging effect during imaging. This technique allows the *in situ* penetration of NP on skin to be observed by SEM. The experiment was done using a Cryo-SEM fitted with a cryo-stage and preparation chamber (Oxford CT-1500 and Philips XL30 SEM, Philips, The Netherlands).

2.4 Coating of vaccines on microprojection array patches

Coating solution containing methylcellulose and Fluvax® 2008 was prepared. A fast nitrogen gas-jet (~ 10 m/s) was used to coat vaccine onto cleaned patches [29]. In this study, we applied the gas-jet to the microprojection patch at an incident angle (α) of 20˚ or 70˚. During coating, the patches were rotated to ensure uniform coating.

The morphology of coated patches was observed by SEM. The coating thickness was determined by comparing the size change of the microprojections before and after coating in the corresponding secondary electron images.

2.5. Quantitative analysis of delivery efficiency of coating

The delivery efficiency of coating was measured by using methyl ^{14}C-OVA as a tracer as previously described [32]. The coating solution contained MC, Fluvax® 2008, and 1 µCi/ml of methyl ^{14}C-OVA. In this experiment, there were six patches in one group.

2.6 Vaccination of mice

To test the stability of the vaccine coating, we coated fifty NPs (4×4 mm) with a commercial influenza vaccine (Fluvax ® 2008) using gas-jet incident angle of 70° and stored them at 23 ºC (Standard deviation: 0.5 ºC) sealed under dry nitrogen (humidity < 1%). The coating solution contained methylcellulose (10 mg/ml), influenza vaccine (54.5 µg/ml of hemagglutinin protein) and trehalose (50 mg/ml). By using ^{14}C-OVA as a tracer, we measured that 248±29 ng influenza vaccine was delivered to each mouse. The storage temperature was following WHO guidelines [33]. Then, at months 0, 1, 2, 3 and 6, ten of the coated patches were used to immunize groups of five C57BL/6 mice. The mice were vaccinated once by applying coated patches to the inner lobe of each ear and held in place for 10 min for the vaccine to diffuse into the epidermis/dermis. One month post immunization, sera were collected and stored at -20 ºC for antibody titer and Hemagglutination-Inhibition (HI) activity measurements. All animal experiments were conducted according to The University of Queensland animal ethics regulations.

2.7 Hemagglutination-Inhibition Assay

Sera from vaccinated mice were treated with receptor destroying enzyme (RDE II, Denka Seiken Co. Ltd.) prior to HI analysis to remove nonspecific inhibitors of agglutination. Samples were diluted 1:10 in RDE and held at 37°C overnight. An equal volume of sodium citrate 1.6% (w/v) was then added and held at 56°C for 2 hr to neutralize RDE activity. The HI test was performed against each of the three purified influenza viruses present in the Fluvax®2008 formulation using chicken red blood cells by established methods adapted to microtiter format [34]. The purified viruses were supplied by CSL, Australia.

3. RESULTS

3.1. Confirmed penetration of microprojections to the epidermal/dermal layers of mouse skin

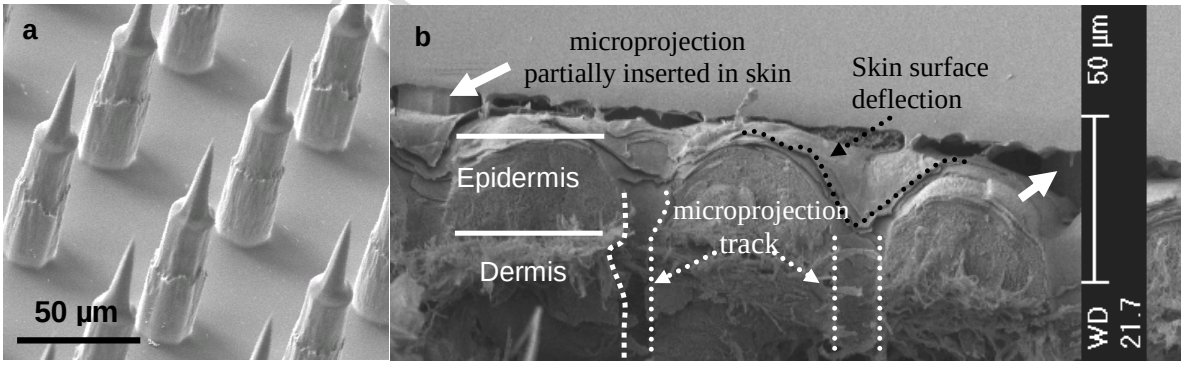

Fig. 1 (a) is an SEM image of uncoated microprojections. (b) shows that microprojections penetrate skin and leave clear needle tracks (shown by the white dotted lines). The black arrow indicates the skin deflection under patch application. The white arrows indicate two microprojections that are not fully in skin.

Fig. 1a shows an SEM image of microprojections which we used in the mouse studies. The length and base diameter of microprojections are 110 and 25 µm, respectively. The spacing between the centres of adjacent microprojections is 70 µm. There are 3364 densely packed microprojections in 4×4 mm area on each patch. Some patches have 0.5 mm edge where there is no microprojection, therefore the total area is 5×5 mm.

To investigate the skin penetration of microprojections, we applied the microprojections to the skin and observed the assembly with Cryo-SEM while the microprojections were still *in situ*. Fig. 1b shows a representative example of the cross section of a NP *in situ* resting on mouse ear skin after being applied by a spring-based device. The white dashed lines in the figure show that the microprojections pierce skin and leave clear needle tracks in the epidermal and dermal layers (the two microprojections were removed during section process). In a separate study, an analysis of the penetration at 130 projection sites showed that the average penetration depth of the microprojections was 42.1±9.9 µm in mouse skin with the same application method [31,35]. The black dashed line indicates the skin surface deflection under patch application. The degree of skin deflection can be affected by many factors – such as microprojection tip sharpness, spacing between microprojections, microprojection length and patch application speed [36]. At the conditions described in this paper, the skin deflection is generally about 20-40 µm, defined by the height difference between the top of skin among microprojections and the edge of the skin puncture hole (from the top to the bottom of the black dashed line). The white arrows indicate two microprojections that are not fully penetrated into the skin.

3.2. Localized coating of vaccine primarily to projection tips

Fig. 2a is an SEM image of uncoated microprojections. The microprojections are composed of 2 parts with different shapes, which in this paper we refer to as the "conical part" (indicated by a black bracket in Fig. 2a) and "cylindrical part" (indicated by a white bracket), respectively. Fig. 2b shows the corresponding back-scattered electron (BSE) image of the uncoated microprojection patches shown in Fig. 2a. As these patches are coated with a thin layer of gold and gold has a high atomic number, they produce bright signal and can be clearly observed on a BSE image. After these patches are coated with organic materials (e.g. DNA, proteins) containing light elements, it is expected that uncoated surface yields less signal on a BSE image. Therefore, BSE images will be used to qualitatively confirm the coating on patches in this study.

We firstly coated patches using the gas-jet incident angle of 20º, which is consistent with that used in previous study [27]. Fig. 2c and 2d show the secondary and backscattered electron images, respectively, of the coated microprojections. Under this coating condition, the whole microprojections were coated and the coating on the surface of the microprojections was very thin (< 50 nm), which is about the resolution of our coating thickness measurement method. On the BSE image, the whole microprojections still produce a bright electron signal, which also qualitatively suggests a thin coating, because the BSE signal from the microprojection surface under the coating layer can still be detected. It took about 3 minutes to coat each individual patch using this condition.

Having confirmed that the microprojections can penetrate skin and the average penetration depth is 42.1±9.9 µm, to increase the delivery efficiency of coated vaccines from the microprojections to skin after penetration, we then set about achieving the coating primarily on the projection tips, compared with the coating on the whole microprojections. We did this by increasing the gas-jet incident angle to 70° and the result is shown in Fig. 2e (secondary electron image) and 2f (backscattered electron image). The SEM results show that the coating became much thicker on the conical part of the microprojections, while it was still thin on the cylindrical part of the microprojections and the base of the patch – in comparison with the coating shown in Fig. 2c and 2d. The coating thickness at the bottom of the conical part was measured to be 0.54±0.05 µm (n=20, indicated by the arrow in Fig. 2e). On the BSE image, the conical part of the coated microprojections produced dark signal as expected when the coating is thick. The very bright BSE signal from both the cylindrical part of the microprojections and the base of the patch qualitatively indicates that the coating on this area is still thin. Under this condition, it took about 5 minutes to coat each individual patch. Because it took longer to finish the coating using this condition, we noted that the solution was resistant to flow on the patches after approximately 4 minutes. At this stage, the use of low gas-jet incident angle could avoid possible thick coating localized in some areas on the base of the patches.

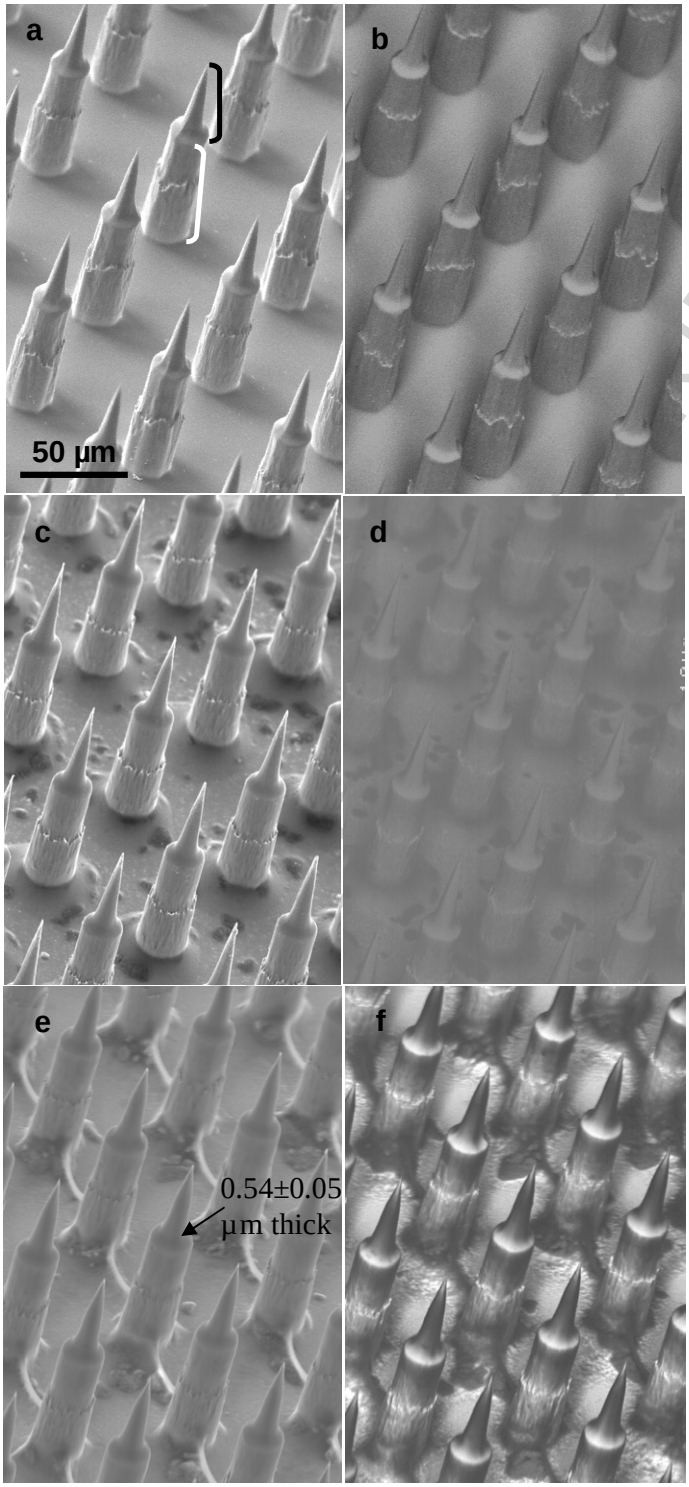

Fig. 2a and 2b are secondary and backscattered electron images of uncoated microprojections, respectively. 2c and 2e are secondary electron images of coated microprojections. Fig. 2d and 2f are corresponding backscattered electron images of the coated microprojections shown in Fig. 2c and 2e, respectively. Fig. 2c-d and 2e-f show the microprojections coated at gas-jet incident angle of 20º and 70º, respectively.

3.3 Quantitative analysis of resultant delivery efficiency following NP application to skin

As shown in Section 3.2, we have manipulated desirable coating morphologies by increasing the incident angle of gas-jet. Here we use the improved coating technique to coat NPs and apply them to the skin to investigate if the coating improvements translate into increased delivery efficiency. In the experiment, we also investigated the possible influence of patch edge on the delivery efficiency. Fig. 3 shows the delivery efficiency of coating under different conditions. First, the benchmark control from previous work [27]: when the patch is 5×5 mm in size (i.e. having 0.5 mm edge around the microprojections, Fig. S1), the delivery efficiency of coating from the patch to skin was only 7.3±1.1%. This delivery efficiency value is not statistically different to our previous work (6.5±0.8% measured by different assay, p=0.55). Second, when we remove the patch edge, the delivery efficiency was increased to 17.8±1.5% even though the coating and patch application conditions remained unchanged from the control group (5×5 mm). Third, using the 4×4 mm patch (Fig. S1), when we increased gas-jet incident angle from 20º to 70º, the delivery efficiency was dramatically further increased to 32.5±3.9%.

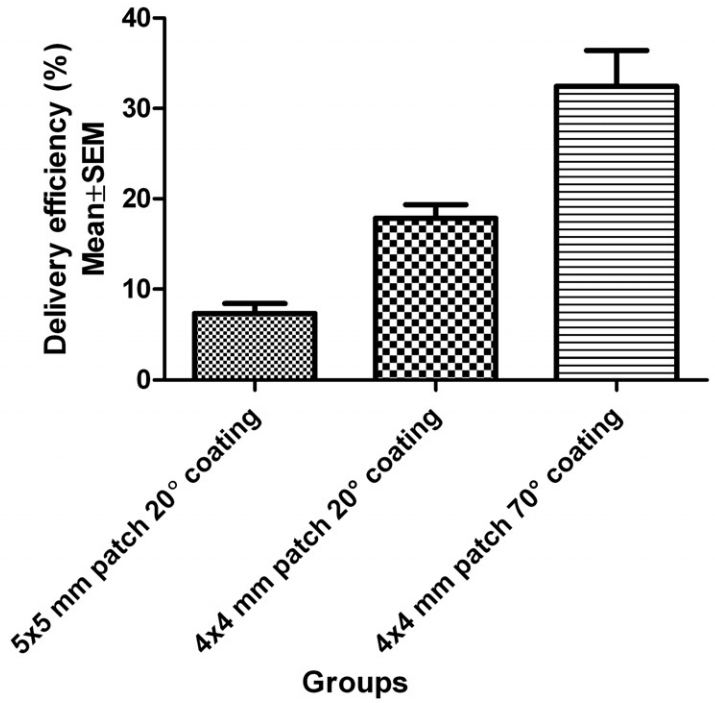

Fig. 3 shows the delivery efficiency of coating under different conditions. The delivery efficiency was measured by using ^{14}C-OVA protein as a tracer in the coating. Six patches per group were used in the experiment.

3.4 Influenza vaccine dry-coated NPs are thermostable at 23 ºC for at least six months

Fig. 4 shows the HI titers induced by influenza vaccine delivered by dry-coated NPs (4×4 mm, coating with gas-jet incident angle of 70°) after different storage times (up to six months) at 23 ºC. Unimmunized mice were used as the negative control, and the HI titers for all three strains were below detection. For the immunized mice, for all three strains, the HI titers induced by coated NPs after different storage time are comparable with those induced by freshly coated patches ($p > 0.05$ for the HI titers comparison with those at Month 0 for all three strains).

3.5 Confirmed penetration of microprojections to the epidermal/dermal layers of pig skin

We have already shown NPs effectively induce protective immune responses, by delivering dry-coated vaccine to mouse ear skin in previous reported work [27]. However, the mouse ear skin is much thinner than human skin – our ultimate vaccination goal. To show that the densely packed microprojection arrays can also deliver coating to a much thicker skin model, we investigated the penetration of the microprojections in pig skin and the result is shown in supplementary Fig. S2. The microprojections are 200 µm long and spaced at 70 µm between projection tips. Fig. S2 clearly indicates that the coating has been delivered to the epidermal and upper dermal layers of the pig skin. The resultant penetration depth of the microprojections in the pig skin is 101.4±20.5 (Mean±SD) µm.

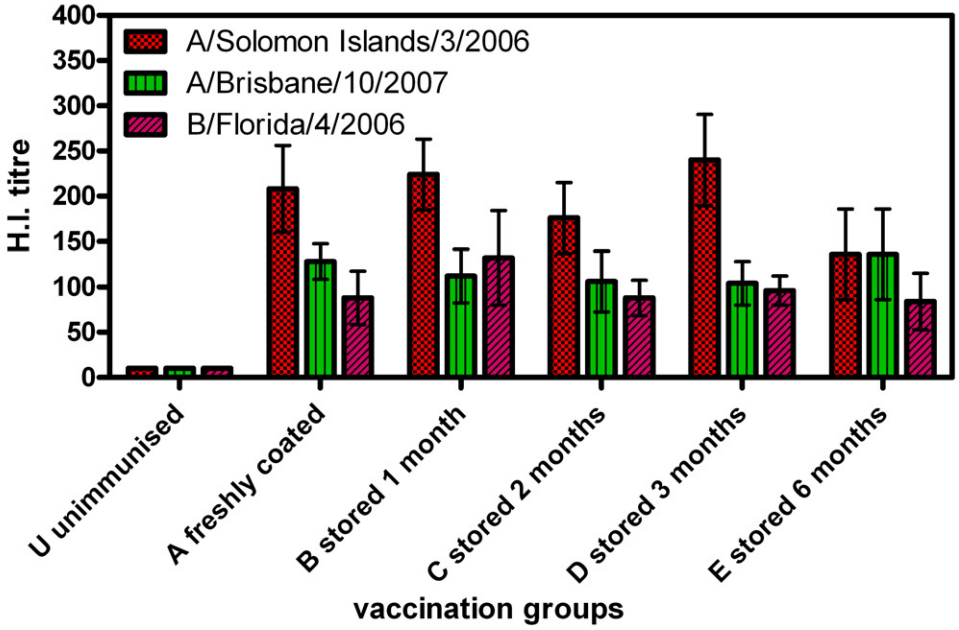

Fig. 4 Immune responses induced by influenza vaccine delivered by dry-coated NPs (*n*=5, the error bars are standard errors of the mean). To test the stability of the vaccine coating, we coated fifty patches with a commercial influenza vaccine (Fluvax 2008®) and stored them at 23 ºC sealed under nitrogen. Then, at months 0, 1, 2, 3 and 6, ten of the coated patches were taken immunizing groups of five C57BL/6 mice. The mice were vaccinated once by applying patches dry coated with Fluvax 2008® (CSL Ltd Melbourne Australia) to the inner lobe of each ear and held in place for 10 min for the vaccine to diffuse into the epidermis/dermis. One month post immunization, sera were collected and stored at -20 ºC for HI activity measurements. Unimmunised mice were used as negative control.

4. DISCUSSION

4.1 Confirmed penetration of the densely packed microprojection arrays in both mouse and pig skin

In this paper, we have studied the *in situ* penetration of microprojections in both the mouse and pig skin. First, in the mouse, we confirmed that the microprojections successfully pierced the stratum corneum and penetrated to the epidermal and dermal layers in mouse skin. However, the penetration of the full length of the microprojections in skin is not achieved, due to the skin deflection and the elastic nature of skin. This is the first time that the cross-sectioned *in situ* investigation of the penetration of microprojections in skin is reported. Our findings are consistent with the previous results obtained by using fluorescent dyes tracking the penetration of microprojections [27,31,32]. For enhanced delivery efficiency of coating, we can either localize the

majority coating on the distal part of the microprojections, or increase the penetration depth of the microprojections (or both).

Our previously-reported results have shown that the densely packed microprojections can directly target the vaccine to thousands of skin's APCs [27]. Associated with this targeted delivery, over 100 times does sparing – compared to the needle – with comparably-protective responses, was achieved in mouse model when delivering influenza vaccine. Looking ahead, the challenge is to successfully translate these attributes to vaccination in humans. In human skin, the density of the characterized APCs is actually comparable with that in mouse skin (e.g. Langerhans cell density is 1052±109 mm^{-2} in mouse skin [37], and 730±60 mm^{-2} in human upper arm skin [38]). If the densely packed microprojections can also deliver vaccine to a large population of APCs in human skin, we expect that the vaccine efficacy can be dramatically enhanced. However, the human skin is much thicker than mouse skin (e.g. mouse ear epidermis is 17.5±2.1 μm [37]; the human forearm dorsal epidermis is 61.3±11.0 μm [39]), so it is necessary to test if the densely packed microprojections can penetrate human skin. In order to test this, we tested the NP penetration into pig skin, because pig is considered as a good model for human skin penetration studies, because pig skin is physiologically similar to human skin both in skin thicknesses and mechanical properties [40]. So, to deliver vaccine to the pig skin, we increased the microprojection length from 110 μm to 200 μm while keeping the momentum of application constant. The results (Fig. S2 and average penetration depth measurement) clearly show that the coating was delivered to the upper dermal layer of the pig skin. Therefore, with proper design of the NP and application device, considering the mechanical properties of the skin, these densely packed microprojections have the potential for human vaccination.

4.2 Improved gas-jet drying coating and removed patch edge result in enhanced delivery efficiency of coating

First, by only removing the patch edge, we increased the delivery efficiency from 7.3±1.1% to 17.8±1.5% – while holding all the coating conditions constant. This increase in delivery efficiency is caused by removing the effect of the patch edge inhibiting penetration. Therefore, by trimming these edges, the projections penetrate further into the skin.

Then, in the gas-jet drying coating process, we found that by increasing the gas-jet incident angle from 20º to 70º, the coating is more localized to the distal part of the microprojections (Fig. 2c-2e) and the delivery efficiency correspondingly increased from 17.8±1.5% to 32.5±3.9% even though the coating and patch application conditions are all the same (4×4 mm patch; gas-jet incident angle of 70° for coating) (Fig. 3). To help provide insights into the mechanism of this improvement, we illustrate the coating process at different gas-jet incident angles in Fig. S3. We assert that the dry-coating attachment to the projections mainly occurs then the coating is separated outside of the coating pool – within the pool, the film on the projections is very thick and more challenging to dry. During the coating process, when we blow the coating solution on one corner of the patch, some of the microprojections will be out of the coating solution pool, as indicated in Fig. S3c-S3f. The viscosity of the thin layer of coating solution adsorbed on the microprojections (out of the coating solution pool) dramatically increases due to fast solvent evaporation under gas-jet, which results in materials being dried onto the microprojections (illustrated in Fig. S3 (c) and (d)). Then we keep rotating the patch so all of the patch microprojections can be coated (Fig. S3 (e) and (f)). Every time when the microprojections are exposed to fast gas-jet, one thin layer of coating will be deposited on their surface. When the gas-jet incident angle is very low (e.g. 20º), nearly whole microprojections (both conical and cylindrical part) will be out of the coating solution pool, so all of these areas are uniformly coated (Fig. S3a). It takes 3 minutes to coat each individual patch.

If we increase the gas-jet incident angle increased from 20º to 70º and blow the coating solution on one corner of the patch, only the distal part of the microprojections will be out of the coating solution pool. Therefore, the coating will be localized on the distal part of the microprojections. Because the surface area of the distal part (conical part) of the microprojections is

much less that of the rest of the microprojections (the surface area of the distal part is only 13% of the total surface area of the microprojections), it takes a longer time (5 minutes) for all of the vaccine to be fully coated. During the extended period of process, more layers of coating are deposited on the distal part of the microprojections, ending up with a relatively thick coating.

The idea – and reduction to practice – of varying the gas-jet incident angle for enhanced vaccine coating on very small and densely packed microprojections is novel. In doing so, we provide a very simple and robust coating method, not only to NPs, but also to the general microneedle vaccine delivery field. Furthermore, our method does not involve repeatable coating of microprojections in the same solution pool, removing the risk of the concentration of different excipients in the solution varying during coating process.

4.3 Thermostability of influenza vaccine coated Nanopatches

The NP is conceptually applicable to a range of vaccines. Here, as a test case, we use a commercial trivalent influenza vaccine (Fluvax® 2008), and show that vaccine dry-coated NPs are stable – inducing comparable immune response – for at least 6 months at 23 ºC. This is important, because it shows that our dry-coating technique can potentially remove the expensive and infrastructure-dependent cold-chain needed for all vaccination campaigns in some temperate regions. In comparison, the estimated shelf life (defined as haemagglutinin content above 2/3 of the original) of trivalent influenza vaccine in liquid form is only 14-20 weeks at 25 ºC [41].

We believe an influenza vaccine is an appropriate test case for the general vaccination field. First, influenza is a major cause of morbidity and mortality, affecting about 20% of the world population at all ages [41]. Second, compared to all current human vaccines, trivalent influenza vaccine has a mid-range stability – therefore it is a good representative of the vaccine stability in general [42]. Third, the immune readout (HI activity) is a widely accepted 'gold standard' used as the surrogate for influenza protective effectiveness in clinical trials [43,44]. Therefore, our thermostabilization work has a direct applicability to clinical medicine.

The improved thermostability of dry-coated influenza vaccine may be due to the addition of stabilizer (trehalose preventing dehydration and conserving the structure of hemagglutinin protein) [45] and the nitrogen atmosphere (preventing oxidation) in the storage condition. However, for a better understanding of the thermostability of our vaccine coated NPs, it is essential for us to conduct further studies at different environment conditions (e.g. temperature, humidity) for different vaccines. Nevertheless, our data clearly reveal that vaccine coated NPs can be stable for a long period of time without refrigeration.

4.4 Large dose sparing

As described (sections 3.2, 3.3 and 4.2), we advance our vaccine coating method, so that the vaccine is more localized to the distal part of the thousands of microprojections on the NP – which penetrate into the skin. In doing so, we demonstrate that 32.5% of the vaccine coated to the device is delivered into the skin. This is a significant advance over our initial pilot study [27], which only delivered ~6.5% of the vaccine on the patch. In addition, the result is important, because it shows that we now achieve equivalent protective immune responses as intramuscular injection (with the needle and syringe), but with only 1/30th of the *actual* dose. It is worth noting that "the $1/30^{th}$ of the *actual* dose per vaccination" is different from the previously reported "$1/100^{th}$ of the skin *delivered* dose needed for one vaccination". In the previous report, the *actual* dose sparing was only around 6 times because of the low delivery efficiency (~6.5%). The 30 times dose sparing is a step change improvement to the field of vaccines: to our knowledge, the highest level of dose sparing achieved with a conventional influenza vaccine using any delivery approach (without relying on an adjuvant) a factor of 10 [46-48]. In the field of influenza vaccine delivery by dry-coated microprojections, the highest dose sparing achieved by others is only 3 times [48].

4.5 Potential utility of NP in low-resource regions

The rollout of vaccines fully to low-resource regions is hindered by many factors including: vaccine affordability; the lack of continuous network of stable, refrigerated storage facilities – i.e. interrupted cold chain; unsafe injections due to needle reuse or use of unsterilized needles; the lack of trained medical practitioners [49-52]. To help address these key constraints affecting so many people in low-resource regions, there is an urgent need for a new vaccine delivery device that is long-term thermostable, efficient, needle-free, simple and affordable.

In this paper, we have introduced NP technology which has the potential to alleviate many of these key problems. First, as one test case, influenza vaccine dry-coated NPs are stable for at least 6 months at 23 ºC, so there is a potential to remove the huge burden of cold chain in vaccination campaign in temperate and subtropical regions [33]. Second, associated with targeted delivery of influenza vaccines to thousands of skin's APCs, the NP achieves unprecedented dose sparing (30 fold). If successfully translated to humans, this dose-sparing will significantly reduce the cost of vaccination – particularly with the more expensive vaccines (e.g. Gardasil; HPV vaccine by Merck). Third, the NPs cannot be re-used in the field, as coating a vaccine is a specialised factory plant activity.

Fourth, we have shown that the NPs can penetrate to the upper dermal layer of the skin only after a significant velocity of application – mitigating the risk of accidental needle-stick injuries that can result in dangerous infections. Fifth, the combined benefits of a compact size (similar to a postage stamp) and no "sharps" are expected to reduce the post-vaccination safe disposal burden.

And finally, the operation of NPs for vaccination is expected to be simple, without the need for specialist training. We achieve this with a simple and economic design NP applicator. Collectively, all of these discussed attributes are important and uniquely position the NP for improving the reach of vaccines to resource-poor regions.

Acknowledgements

The Rutherford Appleton Laboratory (UK; Derek Jenkins) is thanked for the fabrication of the microprojection patches. All members of D^2G^2 are thanked for their inputs. This work was supported by Australian Research Council (DP077464; Prof Kendall's ARC Future Fellowship), National Health and Medical Research Council (#569726, #456150), the Queensland Government (Smart State scheme), Australia and Bill & Melinda Gates Foundation. CSL Ltd is acknowledged for supplying the virus used in the HI assays.

REFERENCES

[1] The World Health Report, http://www.who.int/whr/1996/media_centre/press_release/en/index.html, Accessed 28 January 2011.
[2] L.J. Braun, J. Jezek, S. Peterson, A. Tyagi, S. Perkins, D. Sylvester, M. Guy, M. Lal, S. Priddy, H. Plzak, D. Kristensen, D. Chen, Characterization of a thermostable hepatitis B vaccine formulation, Vaccine 27 (2009) 4609-4614.
[3] A. Kols, J. Sherris, HPV vaccines: promise and challenges. http://www.path.org/files/jsrp13710.pdf, Accessed 28 January 2011.
[4] R. Alcock, M.G. Cottingham, C.S. Rollier, J. Furze, S.D. De Costa, M. Hanlon, A.J. Spencer, J.D. Honeycutt, D.H. Wyllie, S.C. Gilbert, M. Bregu, A.V.S. Hill, Long-Term Thermostabilization of Live Poxviral and Adenoviral Vaccine Vectors at Supraphysiological Temperatures in Carbohydrate Glass, Sci. Transl. Med. 2 (2011) article No. 19ra12.
[5] M.A. Miller, E. Pisani, The cost of unsafe injections, B. World Health Organ. 77 (1999) 808-811.
[6] P.R. Bergstresser, G.B. Toews, J.N. Gilliam, J.W. Streilein, Unusal numbers and distributions of Langerhans cells in skin with unique immunological properties, J. Invest. Dermatol. 74 (1980) 312-314.
[7] T.S. Kupper, Immune and inflamatory process in cutaneous tissues – mechanisms and speculations, J. Clin. Invest. 86 (1990) 1783-1789.

[8] T.S. Kupper, R.C. Fuhlbrigge, Immune surveillance in the skin: Mechanisms and clinical consequences, Nat. Rev. Immunol. 4 (2004) 211-222.
[9] M. Seielstad, Whiffs of selection, Nat. Genet. 26 (2000) 131-132.
[10] R.T. Kenney, S.A. Frech, L.R. Muenz, C.P. Villar, G.M. Glenn, Dose sparing with intradermal injection of influenza vaccine, New Engl. J. Med. 351 (2004) 2295-2301.
[11] M.R. Prausnitz, R. Langer, Transdermal drug delivery, Nat. Biotech. 26 (2008) 1261-1268.
[12] M. Kendall, T. Mitchell, P. Wrighton-Smith, Intradermal ballistic delivery of micro-particles into excised human skin for pharmaceutical applications, J. Biomech. 37 (2004) 1733-1741.
[13] I.S. Ozguney, H.Y. Karasulu, G. Kantarci, S. Sozer, T. Guneri, G. Ertan, Transdermal delivery of diclofenac sodium through rat skin from various formulations, Aaps Pharmscitech 7 (2006) article No. 88.
[14] M. Aqil, A. Ahad, V. Sultana, A. Ali, Status of terpenes as skin penetration enhancers, Drug Discov. Today 12 (2007) 1061-1067.
[15] T. Nochi, Y. Yuki, H. Takahashi, S.I. Sawada, M. Mejima, T. Kohda, N. Harada, I.G. Kong, A. Sato, N. Kataoka, D. Tokuhara, S. Kurokawa, Y. Takahashi, H. Tsukada, S. Kozaki, K. Akiyoshi, H. Kiyono, Nanogel antigenic protein-delivery system for adjuvant-free intranasal vaccines, Nat. Mater. 9 (2010) 572-578.
[16] M. Kendall, S. Rishworth, F. Carter, T. Mitchell, Effects of relative humidity and ambient temperature on the ballistic delivery of micro-particles to excised porcine skin, J. Invest. Dermatol. 122 (2004) 739-746.
[17] P.A. Raju, N. McSloy, N.K. Truong, M.A.F. Kendall, Assessment of epidermal cell viability by near infrared multi-photon microscopy following ballistic delivery of gold micro-particles, Vaccine 24 (2006) 4644-4647.
[18] A.R. Denet, R. Vanbever, V. Preat, Skin electroporation for transdermal and topical delivery, Adv. Drug Deliv. Rev. 56 (2004) 659-674.
[19] M. Wallace, B. Evans, S. Woods, R. Mogg, L. Zhang, A.C. Finnefrock, D. Rabussay, M. Fons, J. Mallee, D. Mehrotra, F. Schodel, L. Musey, Tolerability of Two Sequential Electroporation Treatments Using MedPulser DNA Delivery System (DDS) in Healthy Adults, Mol. Ther. 17 (2009) 922-928.
[20] Y. Zhou, F. Fang, J.J. Chen, H.D. Wang, H.Y. Chang, Z.D. Yang, Z. Chen, Electroporation at Low Voltages Enables DNA Vaccine to Provide Protection against a Lethal H5N1 Avian Influenza Virus Challenge in Mice, Intervirology 51 (2008) 241-246.
[21] S. Babiuk, M. Baca-Estrada, L.A. Babiuk, C. Ewen, M. Foldvari, Cutaneous vaccination: the skin as an immunologically active tissue and the challenge of antigen delivery, J. Control. Release 66 (2000) 199-214.
[22] M. Cormier, B. Johnson, M. Ameri, K. Nyam, L. Libiran, D.D. Zhang, P. Daddona, Transdermal delivery of desmopressin using a coated microneedle array patch system, J. Control. Release 97 (2004) 503-511.
[23] H.S. Gill, M.R. Prausnitz, Coated microneedles for transdermal delivery, J. Control. Release 117 (2007) 227-237.
[24] H.S. Gill, M.R. Prausnitz, Coating formulations for microneedles, Pharm. Res. 24 (2007) 1369-1380.
[25] S. Kaushik, A.H. Hord, D.D. Denson, D.V. McAllister, S. Smitra, M.G. Allen, M.R. Prausnitz, Lack of pain associated with microfabricated microneedles, Anesth. Analg. 92 (2001) 502-504.
[26] A.P. Raphael, T.W. Prow, M.L. Crichton, X.F. Chen, G.I.P. Fernando, M.A.F. Kendall, Targeted, Needle-Free Vaccinations in Skin using Multi layered, Densely-Packed Dissolving Microprojection Arrays, Small 6 (2010) 1785-1793.
[27] G.J.P. Fernando, X. Chen, T.W. Prow, M.L. Crichton, E.J. Fairmaid, M.S. Roberts, I.H. Frazer, L.E. Brown, M.A.F. Kendall, Potent immunity to low doses of influenza vaccine by direct delivery to immune cells in skin, PLoS One (2010) e10266.

[28] J.A. Matriano, M. Cormier, J. Johnson, W.A. Young, M. Buttery, K. Nyam, P.E. Daddona, Macroflux (R) microprojection array patch technology: A new and efficient approach for intracutaneous immunization, Pharm. Res. 19 (2002) 63-70.
[29] X. Chen, T.W. Prow, M.L. Crichton, D.W.K. Jenkins, M.S. Roberts, I.H. Frazer, G.J.P. Fernando, M.A.F. Kendall, Dry-coated microprojection array patches for targeted delivery of immunotherapeutics to the skin, J. Control. Release 139 (2009) 212-220.
[30] A.S. Kask, X. Chen, J.O. Marshak, L. Dong, M. Saracino, D. Chen, C. Jarrahian, M.A.F. Kendall, D.M. Koelle, DNA vaccine delivery by densely-packed and short microprojection arrays to skin protects against vaginal HSV-2 challenge, Vaccine 28 (2010) 7483-7491.
[31] X. Chen, A.S. Kask, M.L. Crichton, C. McNeilly, S. Yukiko, L. Dong, J.O. Marshak, C. Jarrahian, G.J.P. Fernando, D. Chen, D.M. Koelle, M.A.F. Kendall, Improved DNA vaccination by skin-targeted delivery using dry-coated densely-packed microprojection arrays, J. Control. Release 148 (2010) 327-333.
[32] M.L. Crichton, A. Ansaldo, X. Chen, T.W. Prow, G.J.P. Fernando, M.A.F. Kendall, The effect of strain rate on the precision of penetration of short densely-packed microprojection array patches coated with vaccine, Biomaterials 31 (2010) 4562-4572.
[33] M. Zahn, P.W. Kallberg, G.M. Slappendel, H.M. Smeenge, A risk-based approach to establish stability testing conditions for tropical countries, J. Pharm. Sci. 95 (2006) 946-965.
[34] S. Fazekas de St.Groth, R.G. Webster, Disquistitions on original antigenic sin. I. evidence in man, J. Exp. Med. 124 (1966) 331-345.
[35] H.J. Corbett, G.J.P. Fernando, X. Chen, I.H. Frazer, M.A.F. Kendall, Skin vaccination against cervical cancer associated human papillomavirus with a novel micro-projection array, PLoS One 5 (2010) e13460.
[36] L.Y. Chu, S.O. Choi, M.R. Prausnitz, Fabrication of dissolving polymer microneedles for controlled drug encapsulation and delivery: bubble and pedestal microneedle designs, J. Pharm. Sci. 99 (2010) 4228-4238..
[37] W.J. Mulholland, E.A.H. Arbuthnott, B.J. Bellhouse, J.F. Cornhill, J.M. Austyn, M.A.F. Kendall, Z.F. Cui, U.K. Tirlapur, Multiphoton high-resolution 3D imaging of Langerhans cells and keratinocytes in the mouse skin model adopted for epidermal powdered immunization, J. Invest. Dermatol. 126 (2006) 1541-1548.
[38] P.S. Friedmann, Disappearance of epidermal Langerhans cells during puva therapy, Brit. J. Dermatol. 105 (1981) 219-221.
[39] N. Falstiejensen, E. Spaun, J. Brochnermortensen, S. Falstiejensen, The influence of epidrmal thickness of trans-cutaneous oxygen-pressure measurements in normal persons, Scand. J. Clin. Lab. Invest. 48 (1988) 519-523.
[40] A.M. Barbero, H.F. Frasch, Pig and guinea pig skin as surrogates for human in vitro penetration studies: A quantitative review. Toxicol. in Vitro 23 (2009) 1-13.
[41] F. Coenen, J. Tolboom, H.W. Frijlink, Stability of influenza sub-unit vaccine - Does a couple of days outside the refrigerator matter? Vaccine 24 (2006) 525-531.
[42] Summary of stability data for commonly used vaccines and novel vaccine formulations, http://www.path.org/files/TS_vaccine_stability_table.pdf, Accessed 28 January 2011.
[43] D. Hobson, R.L. Curry, A.S. Beare, Wardgard.A, A Role of serum hemagglutination-in hibiting antibody in protection against challenge infection with influenza A2 and B viruses, J Hygiene 70 (1972) 767-777.
[44] D.L. Noah, H. Hill, D. Hines, E.L. White, M.C. Wolff, Qualification of the Hemagglutination Inhibition Assay in Support of Pandemic Influenza Vaccine Licensure, Clin. Vaccine Immunol. 16 (2009) 558-566.
[45] J.P. Amorij, A. Huckriede, J. Wischut, H.W. Frifflink, W.L.J. Hinrichs, Development of stable influenza vaccine powder formulations: Challenges and possibilities, Pharm. Res. 25 (2008) 1256-1273.

[46] J.B. Alarcon, A.W. Hartley, N.G. Harvey, J.A. Mikszta, Preclinical evaluation of microneedle technology for intradermal delivery of influenza vaccines, Clin. Vaccine Immunol. 14 (2007) 375-381.
[47] P. Van Damme, F. Oosterhuis-Kafeja, M. Van der Wielen, Y. Almagor, O. Sharon, Y. Levin, Safety and efficacy of a novel microneedle device for dose sparing intradermal influenza vaccination in healthy adults, Vaccine 27 (2009) 454-459.
[48] F.S. Quan, Y.C. Kim, R.W. Compans, M.R. Prausnitz, S.M. Kang, Dose sparing enabled by skin immunization with influenza virus-like particle using microneedles, J. Control. Release 147 (2010) 326-332.
[49] Immunization against diseases of public health importance, W.H.O. fact sheet Nº288, http://www.who.int/mediacentre/factsheets/fs288/en/index.html, Accessed 28 January 2011.
[50] D.B. Hipgrave, J.E. Maynard, B.A. Biggs, Improving birth dose coverage of hepatitis B vaccine, B. World Health Organ. 84 (2006) 65-71.
[51] J.M. Agosti, S.J. Goldie, Introducing HPV vaccine in developing countries - Key challenges and issues, N. Engl. J. Med. 356 (2007) 1908-1910.
[52] M. Wadman, Efforts to improve vaccine stabilization heat up, Nat. Med. 15 (2009) 1232-1232.

Fig. 1 (a) is an SEM image of uncoated microprojections. (b) shows that microprojections penetrate skin and leave clear needle tracks (shown by the white dotted lines). The black arrow indicates the skin deflection under patch application. The white arrows indicate two microprojections that are not fully in skin.

Fig. 2a and 2b are secondary and backscattered electron images of uncoated microprojections, respectively. 2c and 2e are secondary electron images of coated microprojections. Fig. 2d and 2f are corresponding backscattered electron images of the coated microprojections shown in Fig. 2c and 2e, respectively. Fig. 2c-d and 2e-f show the microprojections coated at gas-jet incident angle of 20º and 70º, respectively.

Fig. 3 shows the delivery efficiency of coating under different conditions. The delivery efficiency was measured by using ^{14}C-OVA protein as a tracer in the coating. Six patches per group were used in the experiment.

Fig. 4 Immune responses induced by influenza vaccine delivered by dry-coated NPs (n=5, the error bars are standard errors of the mean). To test the stability of the vaccine coating, we coated fifty patches with a commercial influenza vaccine (Fluvax 2008®) and stored them at 23 ºC sealed under nitrogen. Then, at months 0, 1, 2, 3 and 6, ten of the coated patches were taken immunizing groups of five C57BL/6 mice. The mice were vaccinated once by applying patches dry coated with Fluvax 2008® (CSL Ltd Melbourne Australia) to the inner lobe of each ear and held in place for 10 min for the vaccine to diffuse into the epidermis/dermis. One month post immunization, sera were collected and stored at -20 ºC for HI activity measurements. Unimmunised mice were used as negative control.

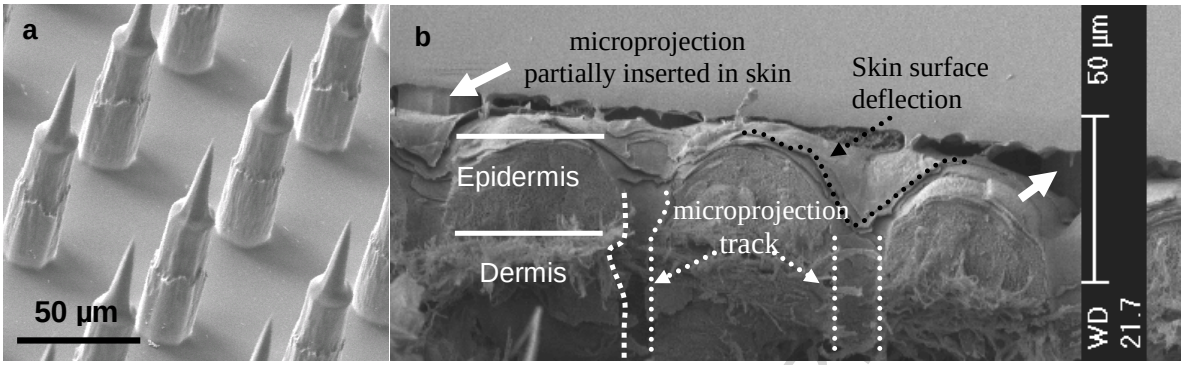

Fig. 1

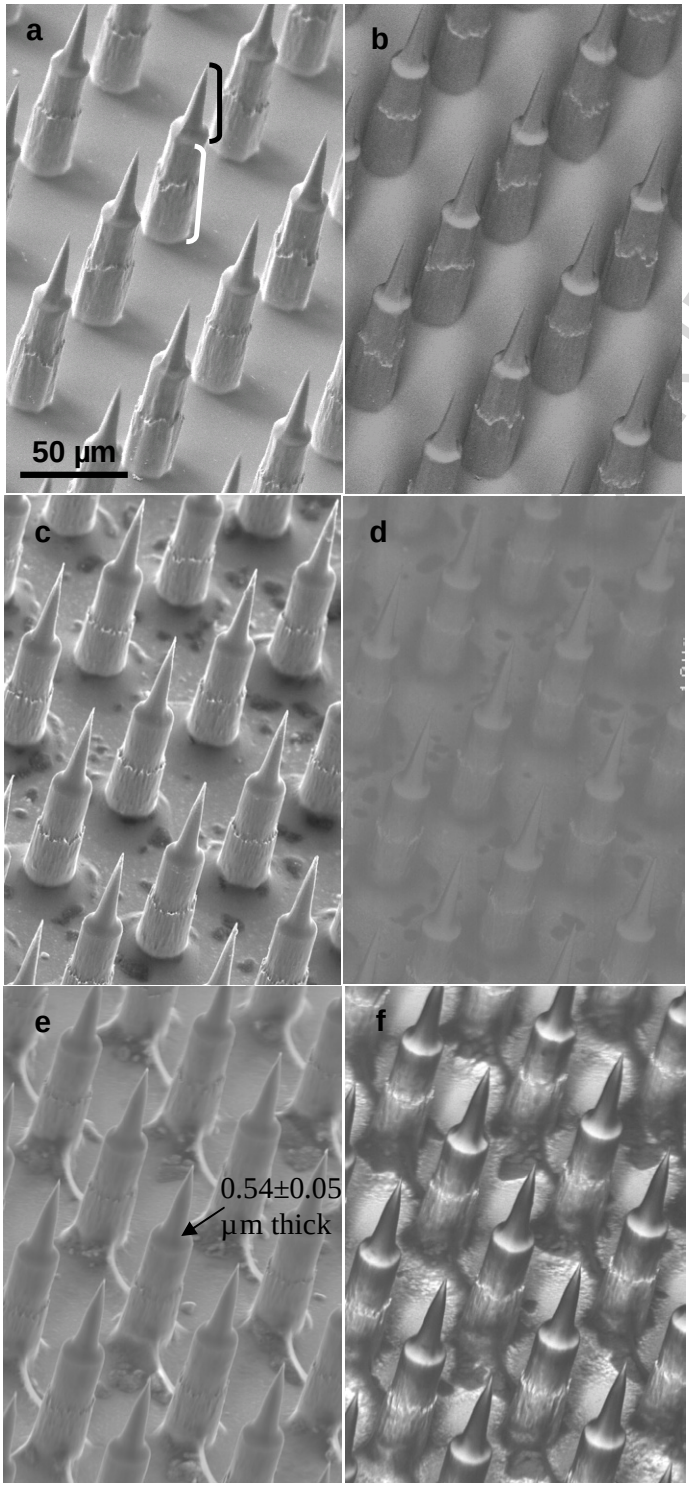

Fig. 2

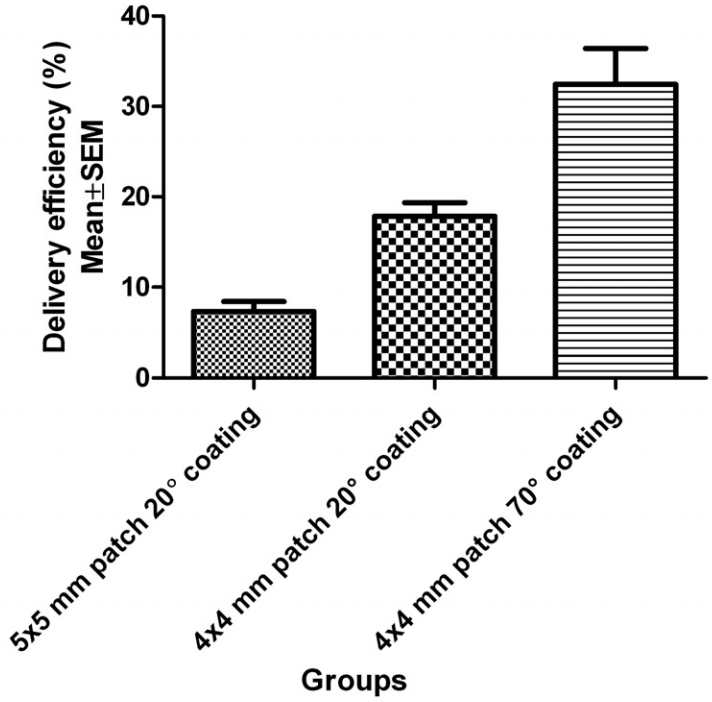

Fig. 3

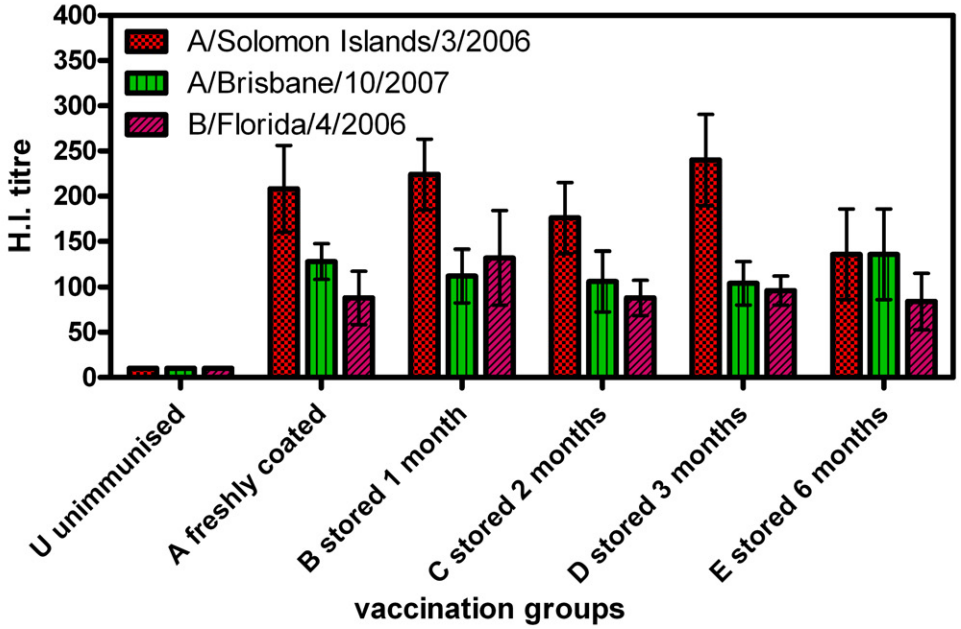

Fig. 4

Graphical Abstract

Improving the reach of vaccines to low-resource regions, with a needle-free vaccine delivery device and long-term thermostabilization

Xianfeng Chen, Germain JP Fernando, Michael L Crichton, Christopher Flaim, Sally R Yukiko, Emily J Fairmaid, Holly J Corbett, Clare A Bover, Alexander B Ansaldo, Ian H Frazer, Lorena E Brown, Mark AF Kendall

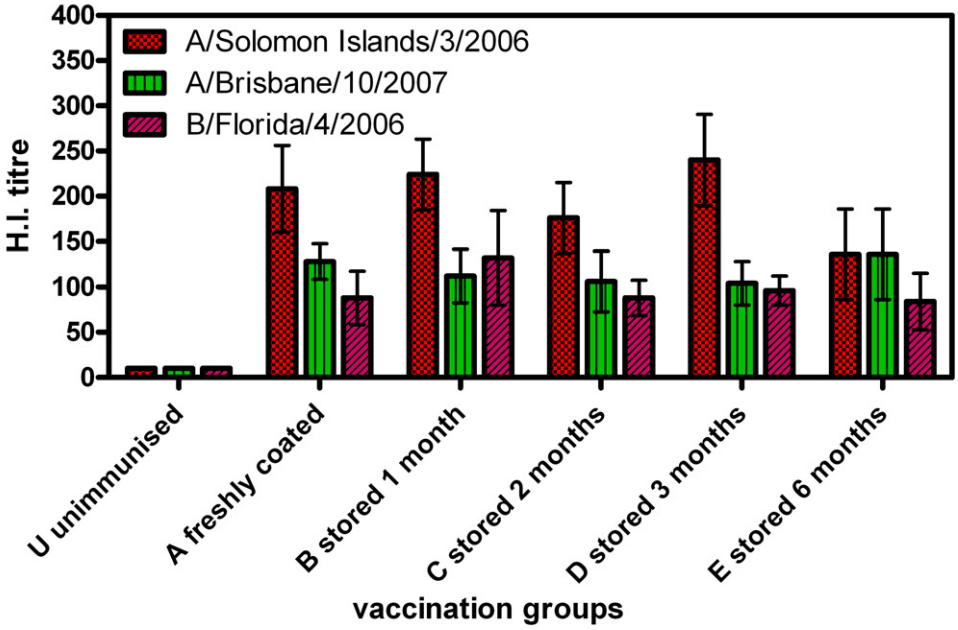

Influenza vaccine coated microprojection patches are stable for at least 6 months at 23 ºC, inducing comparable immunogenicity with freshly coated patches.